Modeling the Circulation of Manila Bay: Assessing the Relative Magnitudes of Wind and Tide Forcing

*Cesar Villanoy and Marilou Martin
Marine Science Institute, College of Science
University of the Philippines
Diliman, Quezon City 1101
E-mail: cesarv@msi01.cs.upd.edu.ph

ABSTRACT

A two-dimensional circulation model of Manila Bay was used to determine the relative importance of wind and tide forcing. Tidal forcing was prescribed using tidal curves based on two diurnal (O_1 and K_1) and two semidiurnal (M_2 and S_2) components on both sides of the bay mouth. A slight amplitude increase towards the head of the bay was obtained, presumably due to shoaling effects. The high correlation between sea level variations at selected coastal tide stations and model results suggests the dependence on tidal forcing at the mouth. Strongest tidal velocities were found at the mouth and decreased towards the head of the bay. The wind-driven component of the flow using mean September 1995 wind forcing shows the presence of two asymmetrical, counter-rotating gyres. Comparison of wind and tidal kinetic energies indicates the dominance of the wind-driven component of the flow only in selected shallow areas adjacent to the coast.

INTRODUCTION

Manila Bay, located along the southwest coast of Luzon (Fig.1), is a very important body of water in the Philippines which is extensively used for various purposes. It harbors the busiest national and international ports in the country and its coast is lined with industrial establishments using Manila Bay waters for industrial purposes either as cooling waters or as waste disposal systems. It also receives discharges from the rivers draining the Central Luzon basin, as well as from Laguna Lake. Despite the huge input of potential water-quality degrading materials, the bay supports a substantial aquaculture and capture fisheries and serves as the main source of livelihood for coastal inhabitants.

The potential fate and transport of the huge amount of material discharged into the bay requires some understanding of the circulation patterns and their variability. Unfortunately, these have been few and far between. Among the early attempts to model the circulation of Manila Bay include those of de las

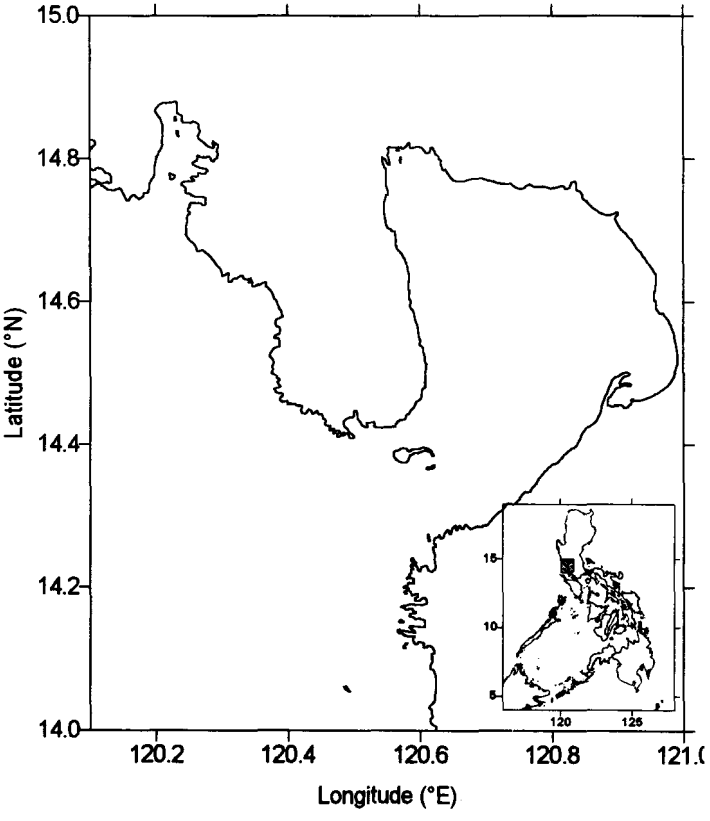

Fig. 1. Location map of Manila Bay.

Keywords: Manila Bay, circulation, tide, wind

**Corresponding author*

Alas and Sodusta (1985) and de las Alas (1987) which considered only the wind-driven barotropic component. In this study, we examine the relative magnitudes of the wind-driven and tidal components in September 1995, where some current measurements are available, and how these magnitudes vary within Manila Bay. A two-dimensional time-dependent circulation model is used in this sudy.

METHODS

Governing Equations

The tidal and wind-driven circulations of Manila Bay were modeled using the shallow-water hydrodynamic equations expressed by:

$$(1)\quad \frac{\partial U}{\partial t}+U\frac{\partial U}{\partial x}+V\frac{\partial U}{\partial y}-fV=-g\frac{\partial \eta}{\partial t}+\frac{\tau_{xs}-\tau_{xb}}{h}+A_H\left[\frac{\partial^2 U}{\partial x^2}+\frac{\partial^2 U}{\partial x^2}\right]$$

$$(2)\quad \frac{\partial U}{\partial t}+U\frac{\partial V}{\partial x}+V\frac{\partial V}{\partial y}+fU=-g\frac{\partial \eta}{\partial t}+\frac{\tau_{xs}-\tau_{xb}}{h}+A_H\left[\frac{\partial^2 V}{\partial x^2}+\frac{\partial^2 V}{\partial y^2}\right]$$

and the equation of continuity:

$$(3)\quad \frac{\partial \eta}{\partial t}=-\left(\frac{\partial U}{\partial x}+\frac{\partial V}{\partial y}\right)$$

where U and V are the vertically-averaged velocities, f is the Coriolis Parameter, η is the bottom depth, η is the sea surface elevation, τ_{xs} and τ_{ys} are the horizontal components of windstress, and τ_{xb} and τ_{yb} are the components of bottom stress. These equations were solved using a leap frog finite differencing scheme over an Arakawa-C staggered grid with a grid resolution of 900m x 900m. The model domain and bathymetry are shown in Fig. 2.

Boundary Conditions

Surface wind stress was prescribed using realistic winds obtained from the Manila PAGASA Station using the following parameterization:

$$(4)\quad \tau_{sx}=\frac{\rho_a C_D W_x\sqrt{W_x^2+W_y^2}}{\rho_w},\tau_{sy}=\frac{\rho_a C_D W_y\sqrt{W_x^2+W_y^2}}{\rho_w},z=0$$

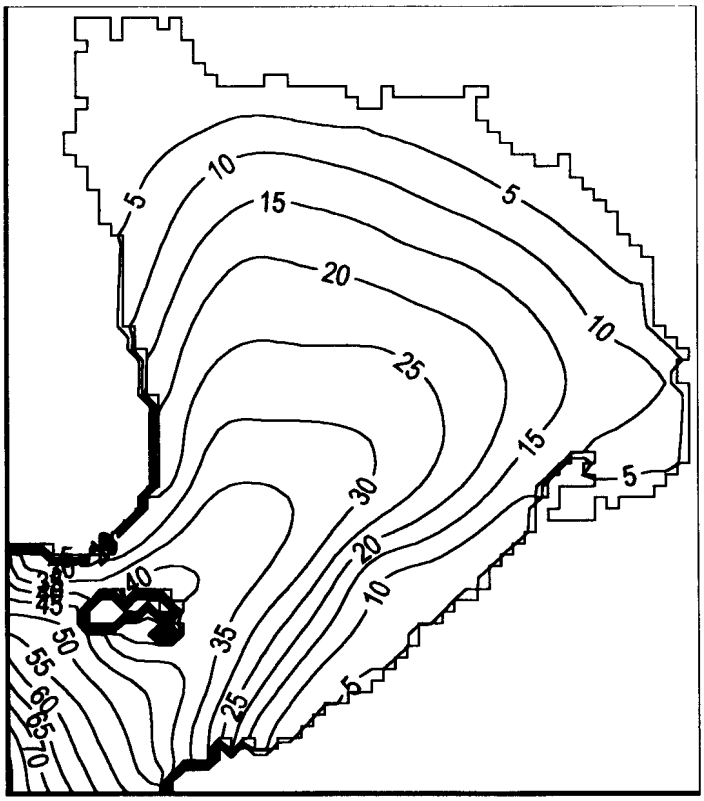

Fig. 2. Model domain and bathymetry.

$$(5)\quad \tau_{sx}=C_B U\sqrt{U^2+V^2},\tau_{sy}=C_B V\sqrt{U^2+V^2},z=h$$

where W_x and W_y are the components of wind speed; C_D and C_B are the surface and bottom drag coefficients, respectively; and ρ_a (=1.2 kgm^{-3}) and ρ_w (=1025kgm^{-3}) are the reference air and water densities. Values of C_D and C_B were based on Large and Pond (1981) and Walsh (1988).

At the model open boundaries, the sea surface elevations were prescribed using tidal harmonics of 4 diurnal (O_1 and K_1) and semidiurnal (M_2 and S_2) components (Fig. 3) calculated from tidal data for two tide stations at both sides of the mouth (NAMRIA 1995). Velocities normal to the open boundary were solved using the linearized forms of equations (1) and (2) while the tangential velocities were set to zero.

The tidal model was allowed to run for a full spring-neap cycle and hourly tidal velocities stored for further analysis. The wind-driven circulation was also simulated by adding wind stress forcing using averaged winds from wind records obtained at the Manila PAGASA Station from August to

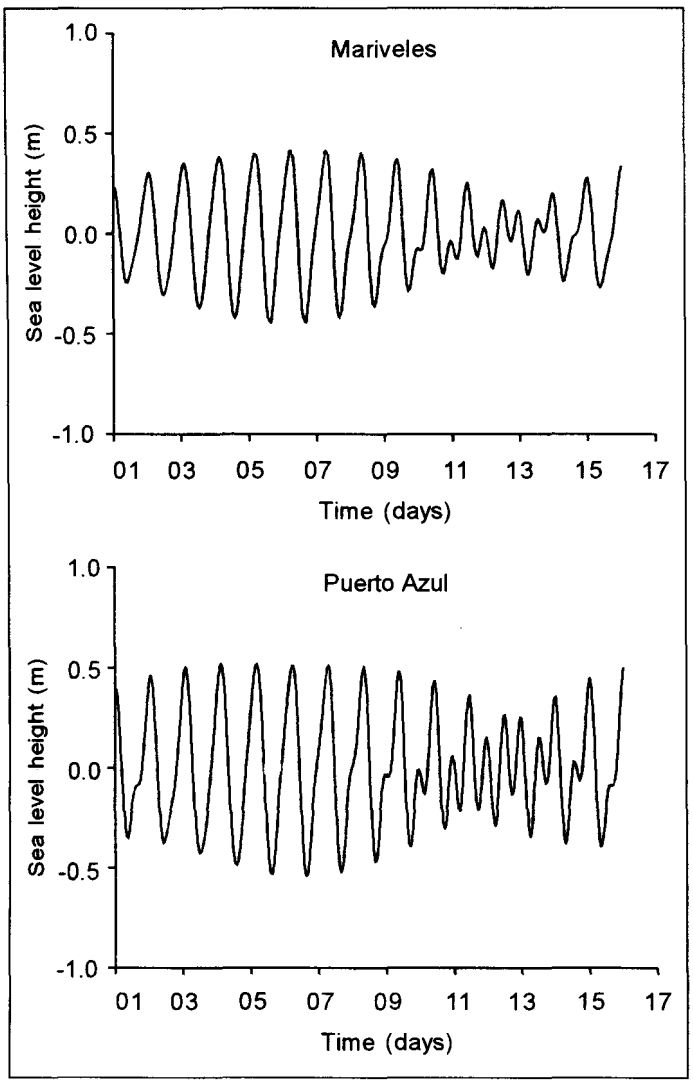

Fig. 3. Tidal curves in Mariveles and Puerto Azul used to force open boundary tides.

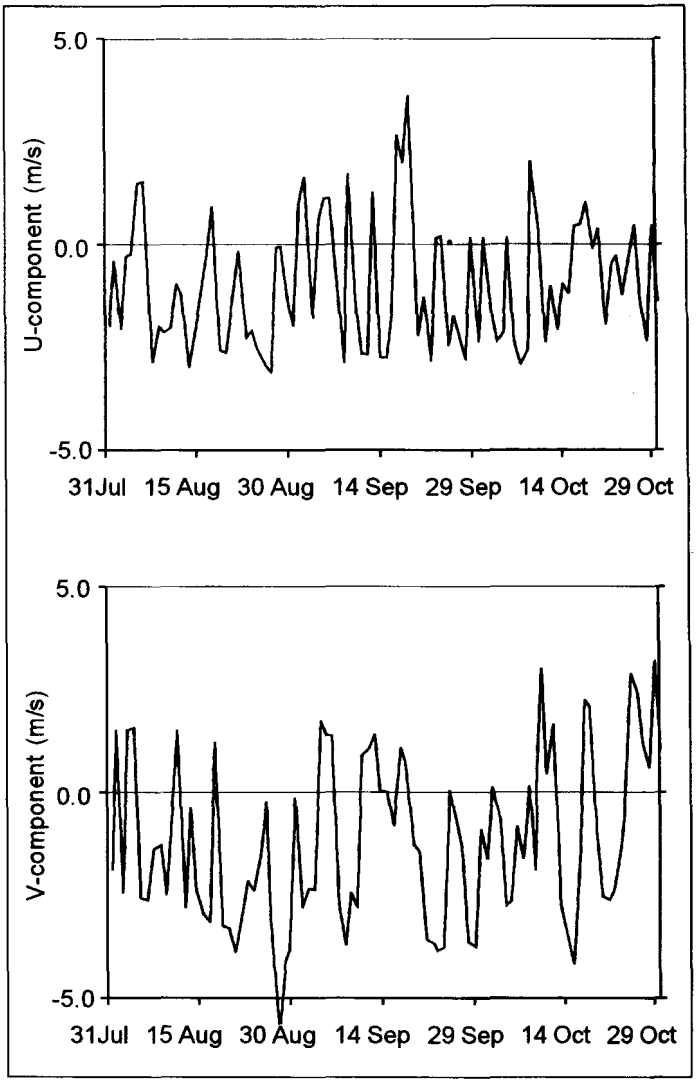

Fig. 4. Wind velocities from the Manila PAGASA Station from July 31 to October 30, 1995

October 1995 (Fig. 4). This particular period was chosen because of the availability of short-term current measurements from the National Power Corporation (NAPOCOR) at two locations near the mouth of the bay.

RESULTS

In a small semi-enclosed area like Manila Bay, the tidal potential is expected to be negligible. Instead, the tidal forcing at the open boundary (e.g., at the mouth of the bay) dominates, as shown by the very similar tidal characteristics at different locations around the bay between predicted tides from available tide tables and modeled sea surface elevations. Fig. 5 shows the correlation between model-derived and measurement-derived tidal characteristics at different tide stations along the coast. The high correlation suggests that the tidal circulation is dominated by the forcing at the boundary.

The co-range plots shown in Fig. 6 show a slight increase in the amplitudes of the four tidal components towards the head of the bay and into the shallow area off the Pampanga River, presumably due to shoaling effects. Progression of the tide as it enters into the bay starts in the southern part of the mouth (between Corregidor Island and the Cavite coast) and proceeds towards the northwestern section of the Bay.

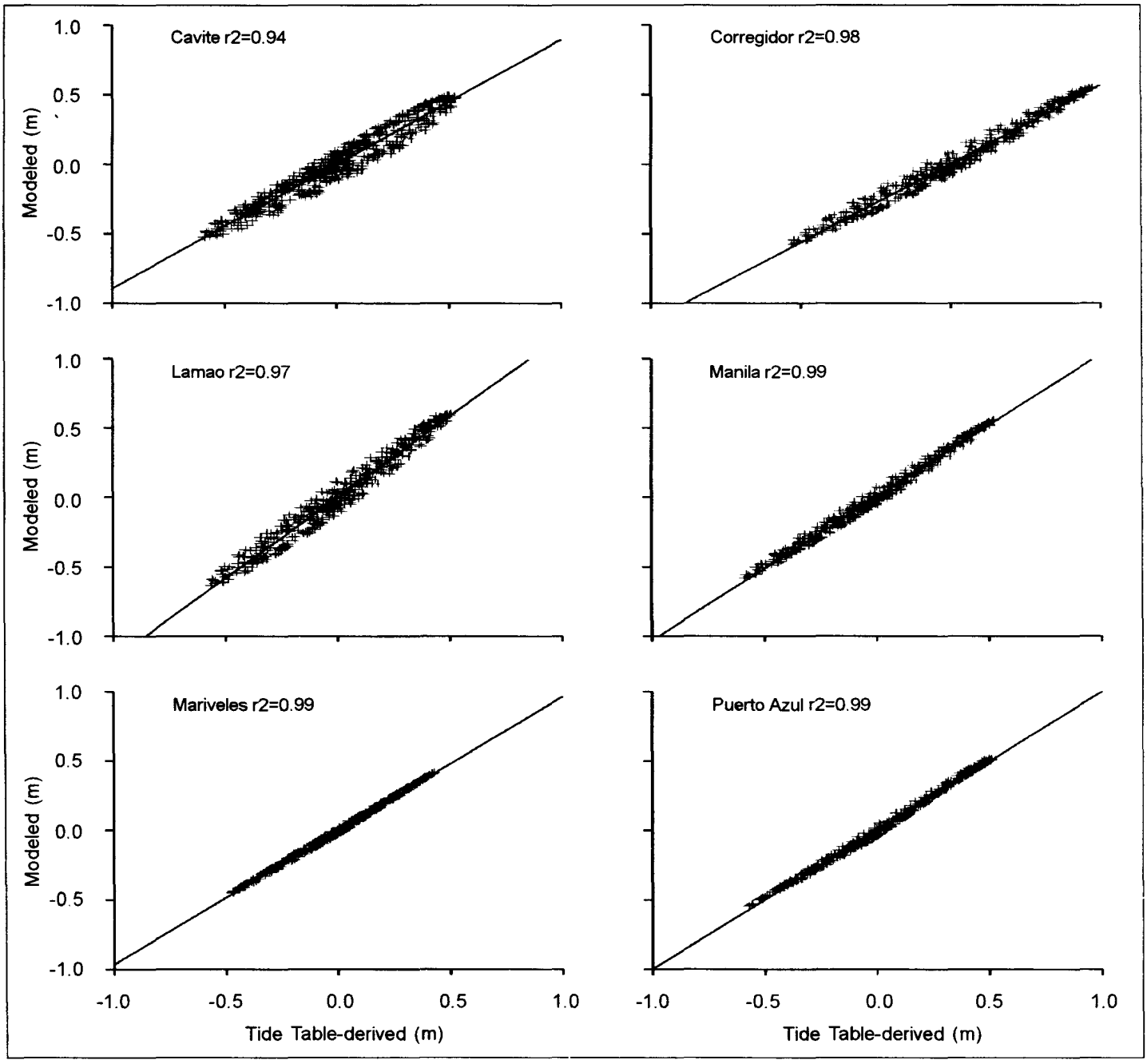

Fig. 5. Correlation between tide table-derived and modelled tidal elevations.

The tidal ellipses calculated using the model velocities are shown in Fig. 7. Tidal advection near the mouth can extend to over 5 kms over a tidal cycle while at the head of the bay, tidal advection is weak. The implications of these are that flushing of material out of the bay will be unlikely if the tidal advection scale is less than the distance towards the bay mouth where offshore currents may transport it away into the open sea. The tidal velocities are maximum at the mouth with magnitudes of >0.5 ms-1. The residual tidal velocity is strongest at the mouth where it enters the bay north of Corregidor and exits to the south (Fig. 8).

The wind velocities obtained from PAGASA for the period August-October, 1995 were predominantly southwesterly but

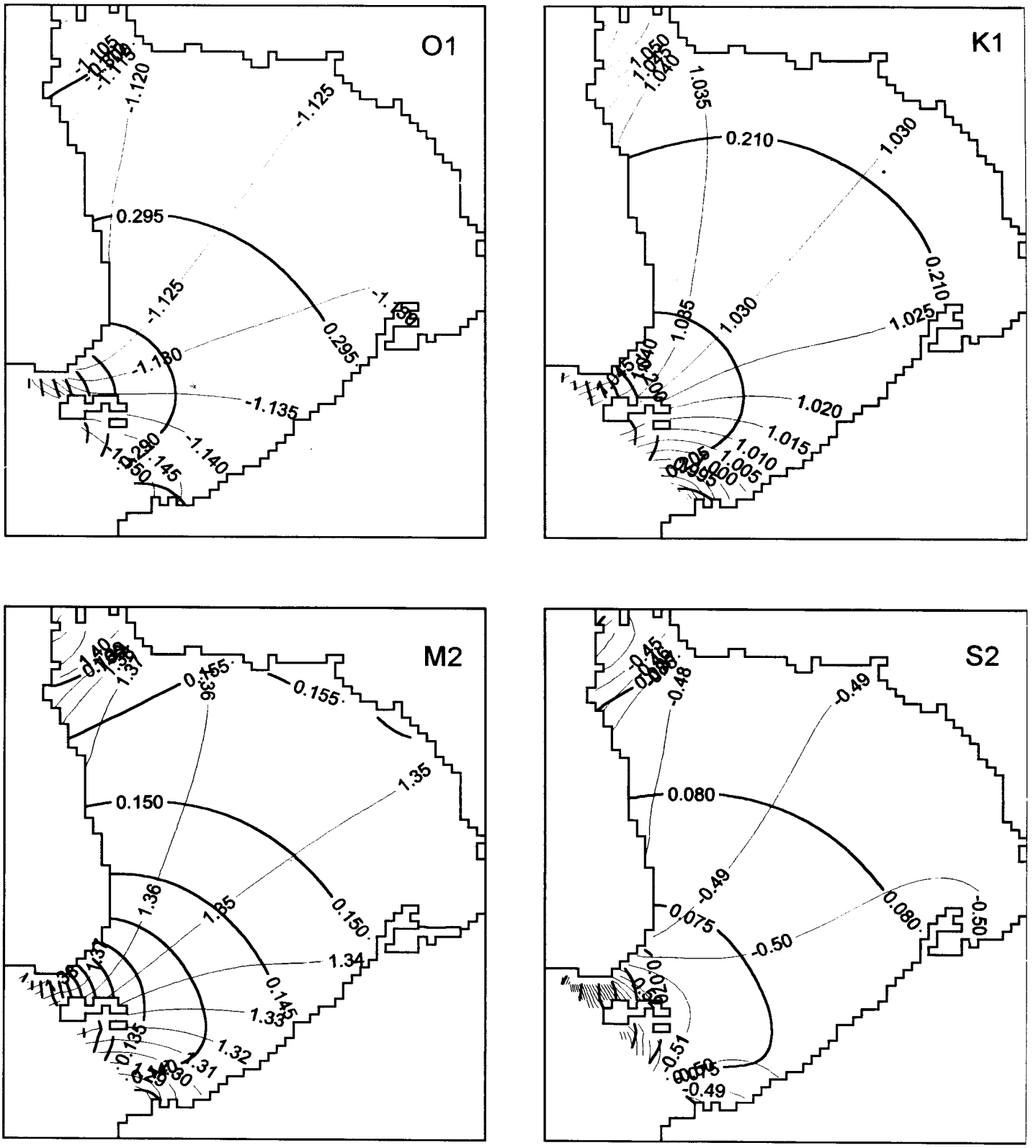

Fig. 6. Relative co-phase (thin lines) and co-range (dark lines) plots for four different tidal components in Manila Bay.

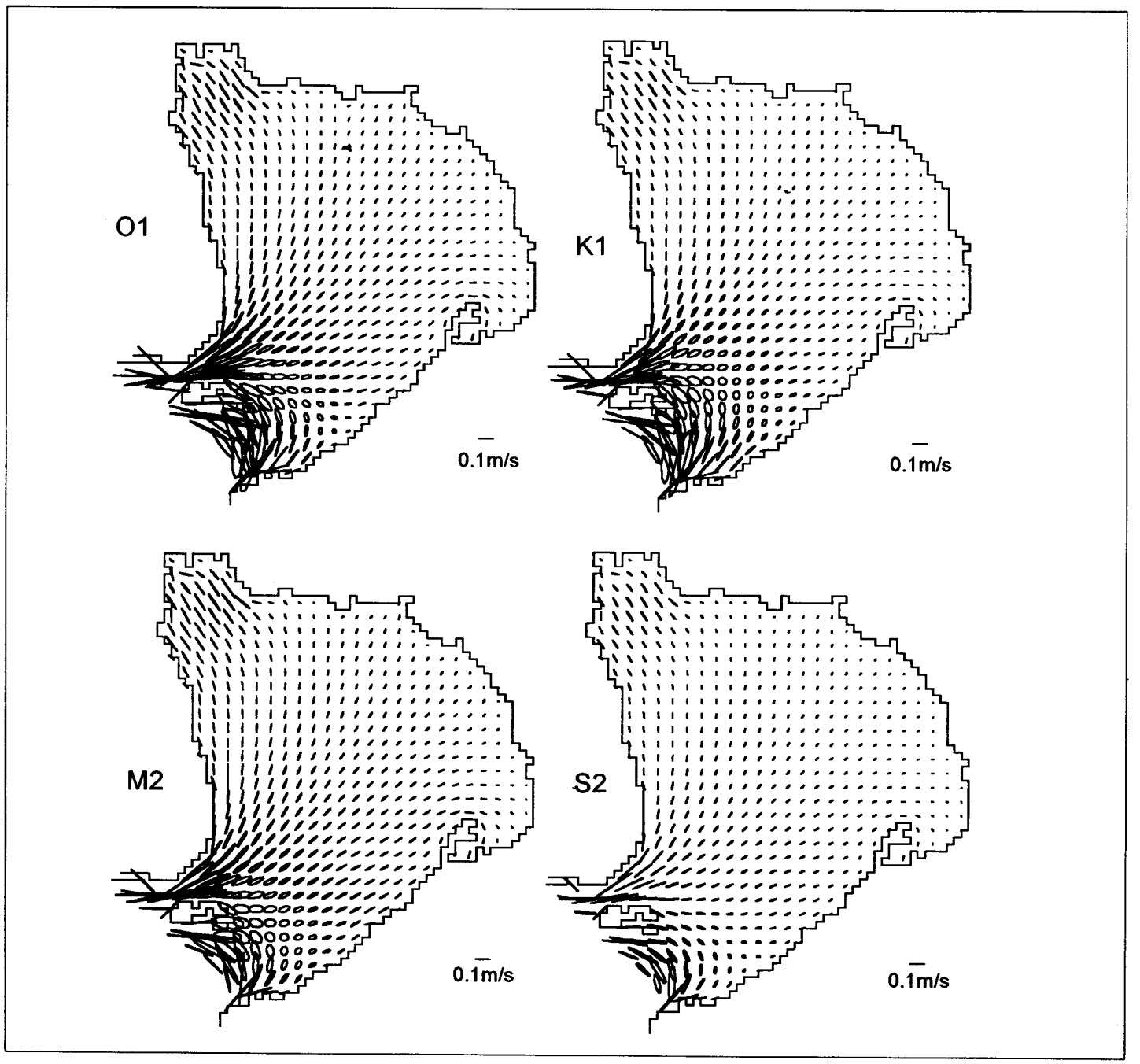

Fig. 7. Tidal ellipses of Manila Bay tides.

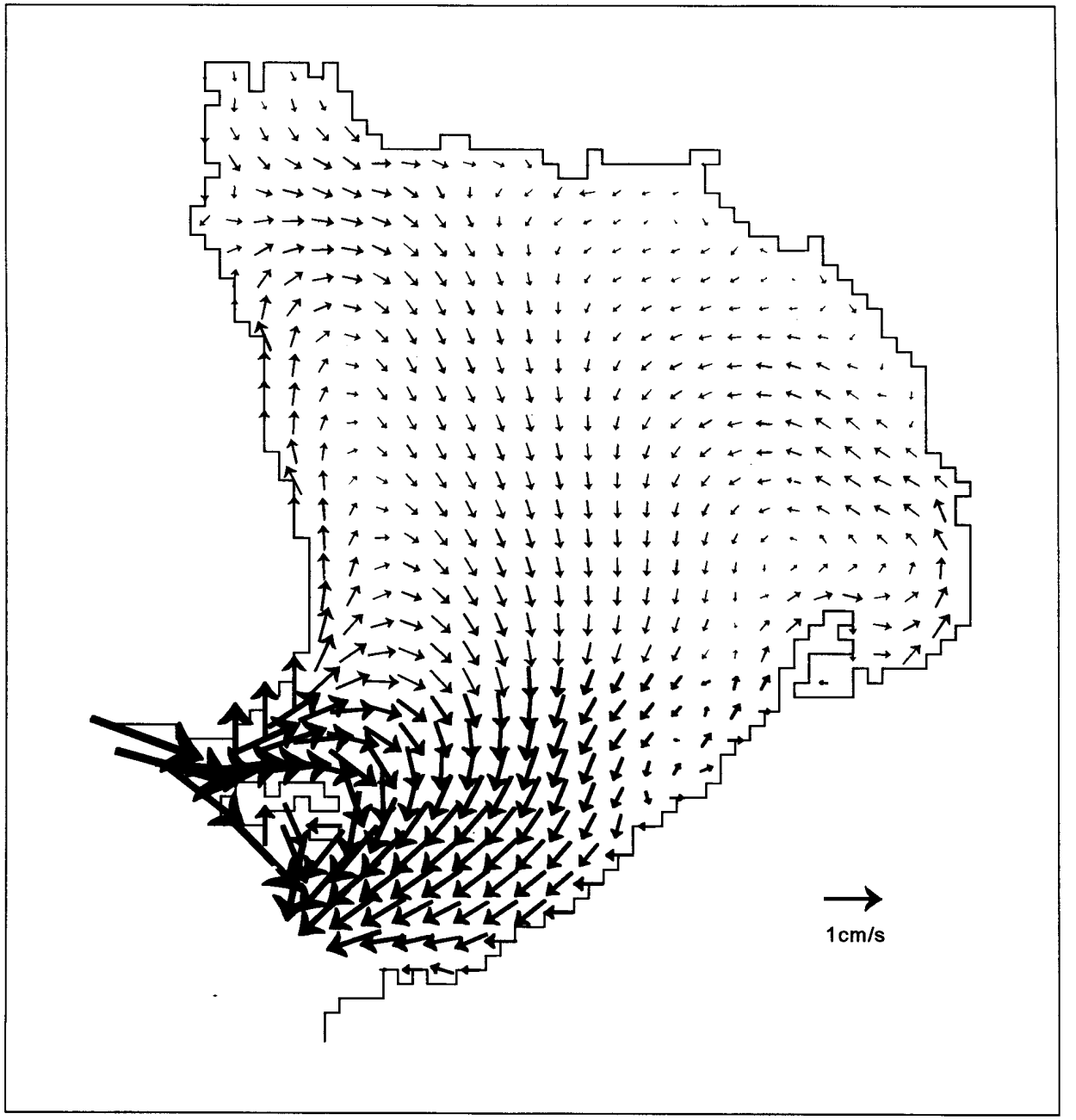

Fig. 8. Residual tidal velocities.

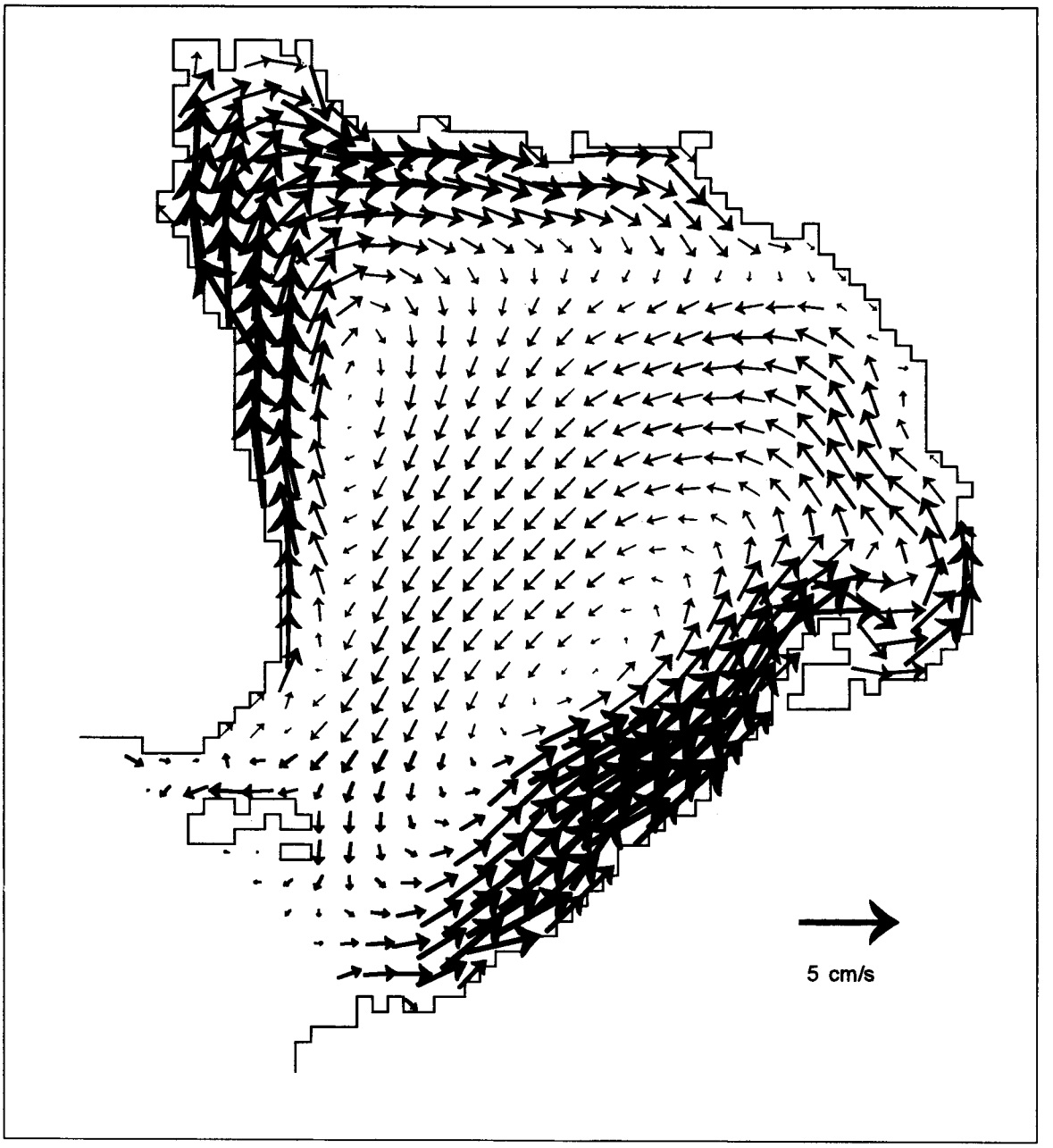

Fig. 9. Simulated wind-driven velocities for southwesterly winds.

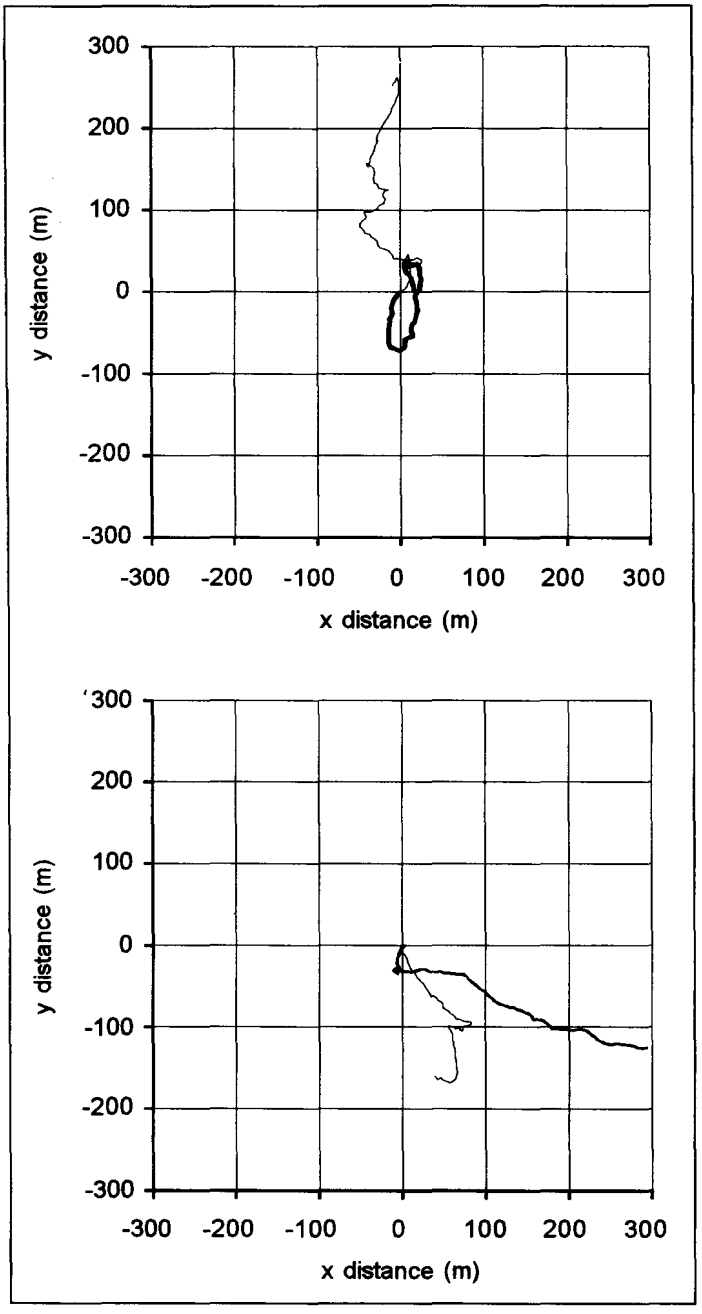

Fig. 10. Progressive vector diagram of current measurements in Corregidor (top) taken on September 7, 1995 and off Ternate (bottom) taken on September 8, 1995 at 5m (thin line) and 10m (thick line) depths (source: NAPOCOR).

were characterized by gusts that can change direction and can persist for a few days. Using southwesterly winds, the model results show that adjacent to the coast, the transport of water is along the direction of the wind. The accumulation in the head of the bay will result in a return flow in the interior of the bay as shown in Fig. 9. Topographic variations, however, do not result in a symmetrical flow pattern. Instead, the alongshore flow on the western coast of the bay lies just adjacent to the offshore return flow. This is not the case for the eastern part where the flows are broader. In the interior of the bay is a weak anticyclonic circulation with a smaller cyclonic gyre in the eastern part of the bay off Cavite.

Current meter records over a period of two days at two different locations are shown in Fig. 10 as progressive vector diagrams. Note that the limited data available is insufficient to do any kind of quantitative comparison between the model and observations. Longer term measurements should be conducted in order to obtain an adequate amount of data for model calibration purposes. However, there appears to be some similarities between flow patterns off Corregidor and Ternate. For instance, the currents off Ternate show a net westward flow consistent with the wind-driven model results, while off Corregidor, the currents have a stronger tidal oscillation.

DISCUSSION

At different locations around the bay, the effects of the tides and wind-driven currents can vary depending on the bathymetry and distance from the mouth. Determining the relative magnitudes of both forcing functions was conducted by calculating the total kinetic energy per unit area based on the following formulation (Gill 1982):

$$(6)\quad K = \frac{1}{2}\rho_w h\left(U^2 + V^2\right)\Delta x \Delta y$$

The total kinetic energy per unit area for the peak flood and ebb currents during spring and neap tides are shown in Fig. 11. Highest kinetic energy is found at the mouth with the interior of the bay averaging about 5.0×10^6 J. The variation of total kinetic energy between spring and neap tides do not appear to be significant. On the other hand, the total kinetic energy of the wind-driven component of the circulation (Fig. 12, upper plot) is weaker compared to the tidal component. In the deep sections of the bay, kinetic energy is only about one

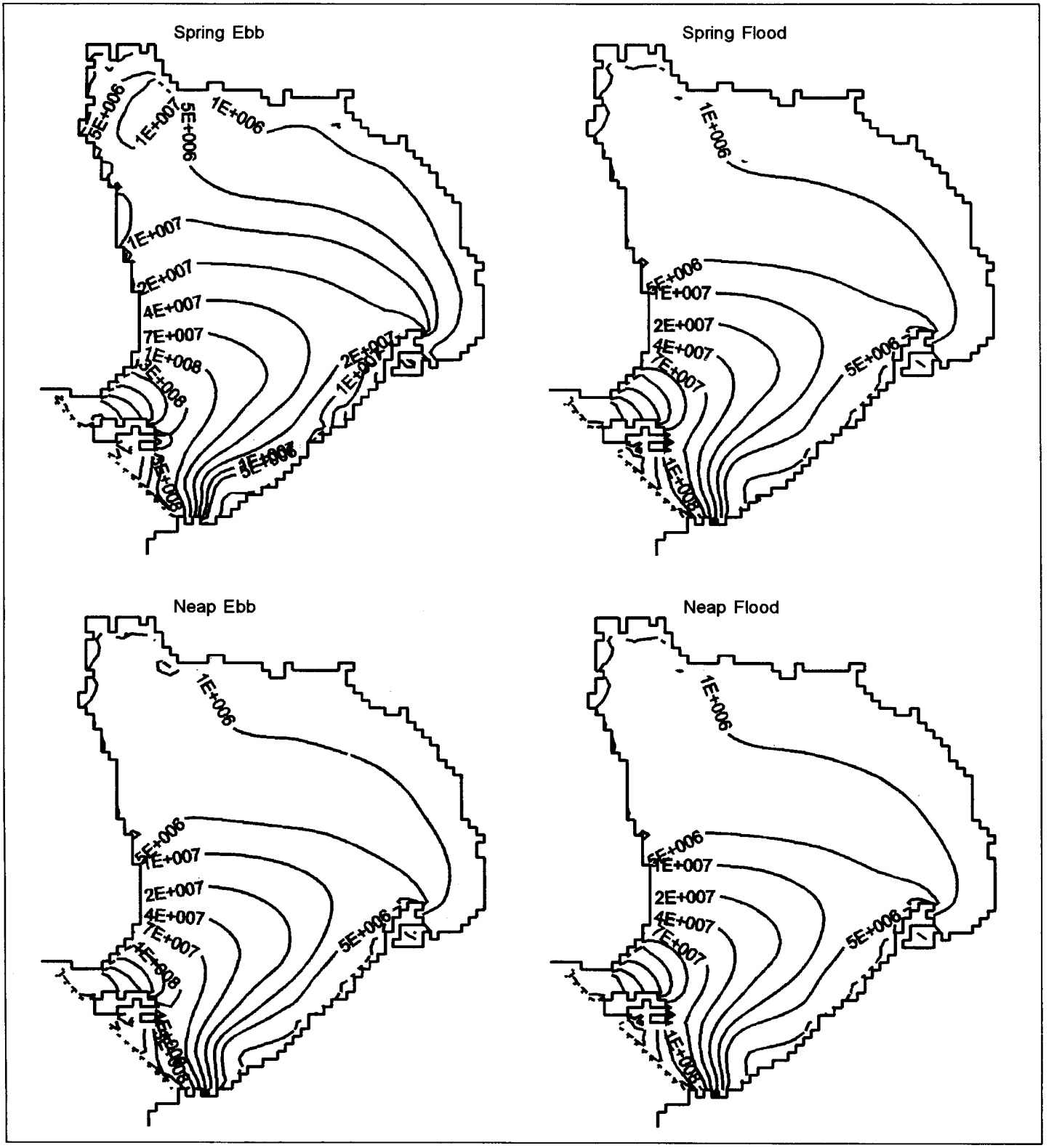

Fig. 11. Kinetic energy (in joules per unit area) at different tide phases.

Fig. 12. Kinetic energy (in joules) for wind-driven circulation (a) and ratio between the spring ebb kinetic energy and wind-driven kinetic energy (b). Shaded areas represent ratios < 1.

third of the tidal kinetic energy. The lower plot in Figure 12 shows the ratio between the kinetic energy of the tidal currents with those of the wind-driven currents. The shaded portions indicate areas where the ratios are less than one and hence represent areas where wind-driven effects dominate.

The results presented here were based on simulation runs conducted for only a limited period of the year. As the Philippines experiences strong monsoonal variations, it is expected that the wind driven component of the Manila Bay circulation will exhibit such large variations as well. Understanding such variations will require long term current measurements and will prove to be essential in understanding the transport patterns of potential pollutants in the bay.

CONCLUSIONS

Simulation of the tidal and wind-driven circulation in Manila Bay during September 1995 indicates that circulation is essentially dominated by the tides except in some shallow areas adjacent to the coast where wind forcing is greater or at least of the same order of magnitude as the tidal forcing. The strongest tidal currents are found at the bay mouth with speeds in excess of 0.5m/s during peak flood and ebb flow and tidal advection length scales of about 5 km. The dominance of tidal advection in the interior of the bay will have some implications on bay flushing, since advection length scales decrease towards the head of the bay where most of the pollutants are being discharged.

ACKNOWLEDGMENTS

The authors wish to acknowledge the Office of Research Coordination (ORC) of the University of the Philippines for providing the opportunity to present this study at the "Symposium on Pollution in Manila Bay: Asssessments and Solutions," 12 Feb 1997, College of Science. The computer simulations were done at the Research Computer System of the College of Science, University of the Philippines. Acknowledgment is also due the National Power Corporation for providing the current meter data used in this study and J. G. de las Alas for reviewing the manuscript.

REFERENCES

de las Alas, J.G., 1990. Estimation of sedimentation rate in Manila Bay. In H. T. Yap, M. Bohle-Carbonell, & E. D. Gomez (eds.), Oceanography and Marine Pollution: An ASEAN-EC Perspective. Marine Science Institute, University of the Philippines. 384 pp.

de las Alas, J.G. & J. A. Sodusta, 1985. A model for the wind-driven circulation of Manila Bay. *Nat. Appl. Sci. Bull.* 37: 159-170.

Gill, A. E., 1982. Atmosphere-ocean dynamics. Academic Press Inc., California, 662 pp.

Large, W.G. & S. Pond, 1981. Open ocean momentum flux measurements in moderate to strong winds. *J. Phys. Oceanogr.* 11: 324-336.

NAMRIA, 1995. Tide and Current Tables 1995. National Mapping and Resource Information Authority, Department of Environment and Natural Resources, 238 pp.

Walsh, J. J., 1988. On the nature of continental shelves. Academic Press Inc., California, 520 pp.